On new scalings in a temporally evolving turbulent plane jet using a different and physical choice of equivalence transformations

Michael Frewer

On new scalings in a temporally evolving turbulent plane jet using a different and physical choice of equivalence transformations

A comment to J. Fluid Mech. (2018), **854***, pp.233-260 by Sadeghi et al.*

Michael Frewer*

Heidelberg, Germany
October 4, 2018
(Update: December 5, 2018)

1. Abstract and Summary

By choosing a different but physically consistent set of equivalence transformations than the inconsistent one proposed by Sadeghi *et al.* (2018), it will be shown how for a temporally evolving plane jet the numerically computed statistical profiles up to second moment can be correctly scaled such as to collapse into a single invariant profile.

In contrast to the claims made in Sadeghi *et al.* (2018), the algorithm developed therein and then re-iterated herein, is no prediction algorithm as how turbulent jet flow scales. It only is a sophisticated post-processing algorithm to find within a trial-and-error process the appropriate scalings such that numerically computed profiles collapse approximately into a single profile. The algorithm is not able to predict the functional structure of these singly collapsed profiles, not even approximately. The reason is that although the algorithm is based on a systematic Lie-group invariant analysis for the statistical equations of a temporally evolving turbulent jet flow, these equations are unclosed, and so are their invariant transformations. Hence, when performing any invariant analysis on such an infinite hierarchy of unclosed moment equations, it will predominately result into a non-unique solution involving arbitrary functions for which from the outset it is not clear how to specify them. The closure problem of turbulence cannot be circumvented by just employing the method of Lie-group invariant analysis alone, since the arbitrariness just gets shifted from one function to another (see also e.g. Frewer *et al.* (2014*a*) and Frewer & Khujadze (2016)). Hence, without modelling these unclosed equations, an *a priori* prediction as how turbulence scales is and will not be possible. Only *a posteriori*, by anticipating what to expect from numerical or experimental data, the adequate invariant scalings can be generated through an iterative trial-and-error process as shown here in this comment once again.

Also, just because of this arbitrariness involved, one has to be aware of the associated problem that unphysical invariant transformations might get generated once making a certain choice. Hence, it is important to have a physical guideline as how to make a physically sound choice. One such guideline is the classical principle of cause and effect, namely that any statistical invariance must have a cause in the underlying instantaneous Navier-Stokes equations, where the cause itself, however, need not to be an invariant. This guideline will play a central role in this comment (for theoretical details, please see e.g. Frewer *et al.* (2015, 2016) and Appendix A in Frewer *et al.* (2017)) — a guideline which again is intentionally and wittingly missing in Sadeghi *et al.* (2018), with the result that therein again unphysical and inconsistent invariances get generated. Even when formally considering the statistically infinite hierarchy of unclosed moment equations, the still existing connection to the deterministic and instantaneous Navier-Stokes equations may not be ignored, simply because it are these equations which due to their spatially nonlocal and temporally chaotic behavior induce the infinite hierarchy of statistical equations, and not vice versa. Those who generate statistical invariances without establishing a connection to the underlying Navier-Stokes equations act grossly negligent, like again in Sadeghi *et al.* (2018), who even justify their unphysical and inconsistent analysis with the bold statement: "These symmetries are denoted statistical symmetries and they have no direct counterpart in the Navier-Stokes equations" (p.239).

*Email address for correspondence: frewer.science@gmail.com

Two points are to be noted here: Firstly, due to the unclosedness of the statistical moment equations, the invariant transformations derived herein are only equivalence transformations and not symmetry transformations as incorrectly denoted in Sadeghi *et al.* (2018). It is not a semantic sophistry to carefully distinguish between equivalence and symmetry transformations, because in the latter, when applied to a certain set of differential equations, solutions get mapped to solutions of the same set of equations again, while the former acts in a weaker sense, where the considered set of equations get mapped to a different set of equations of the same class. In other words, equivalence transformations do not allow for the same insight into the solution structure of differential equations as symmetry transformations do — see e.g. Frewer *et al.* (2014*b*) for a detailed discussion.

Secondly, the invariance analysis presented herein is only performed up to the second moment in the statistical hierarchy. As in Sadeghi *et al.* (2018), statements about the scaling behaviour of higher order moments are not made, so it cannot be ruled out that the scaling which works for second order also works for higher order moments. This important consistency check remains pending, in particular as the DNS data for higher order moments are not yet at disposal. The data used in this comment is taken from Sadeghi *et al.* (2018) and has been extracted by WebPlotDigitizer.

Finally, this comment will close with Sec. 5, which in detail will reveal the flaws and problems the study Sadeghi *et al.* (2018) faces. The content of that section will not only invalidate their study, but will also serve as a note to directly compare with the correct approach presented herein.

2. Statistical equivalences for a temporally evolving turbulent plane jet

Considered is the 1-point defining set of unclosed turbulent transport equations up to second moment in the inviscid limit ($\nu = 0$) (see Sadeghi *et al.* (2018) for all details)

$$\left.\begin{aligned} \partial_t \overline{U}_1 + \partial_{x_2} H^0_{12} &= 0, \\ \partial_t H^0_{ij} + \partial_{x_2} H^0_{ij2} + \partial_{x_2}(\delta_{i2}\overline{PU_j}^0 + \overline{PU_i}^0\delta_{j2}) - \Phi^0_{ij} &= 0, \end{aligned}\right\} \tag{2.1}$$

where $\overline{U}_1$ is the mean streamwise velocity field of this inviscid and temporally evolving plane jet, $\overline{PU_i}$ its pressure-velocity correlation, and

$$H^0_{ij} = \overline{U_i U_j}, \qquad H^0_{ijk} = \overline{U_i U_j U_k}, \qquad \Phi^0_{ij} = \overline{P(\partial_{x_i} U_j + \partial_{x_j} U_i)}, \tag{2.2}$$

the second and third instantaneous velocity moments and the pressure-rate-of-strain tensor of the jet, respectively. The superscript '0', as defined in Sadeghi *et al.* (2018), indicates that we are dealing here with a 1-point and not a spatially 2-point statistics, i.e., in which for all fields the 2-point correlation distance $\mathbf{r}$ has been set to zero in the limit $\mathbf{r} \to 0$. The four *non-zero* instantaneous double-velocity moments are related to the Reynolds stresses as (*Eqs. (3.2)-(3.5)* in Sadeghi *et al.* (2018))

$$H^0_{11} = R^0_{11} + \overline{U}_1^2, \qquad H^0_{22} = R^0_{22}, \qquad H^0_{33} = R^0_{33}, \qquad H^0_{12} = R^0_{12}. \tag{2.3}$$

Performing a systematic equivalence analysis on (2.1) by using, for example, the Lie software package 'DESOLV-II' by Vu *et al.* (2012), one obtains, in contrast to the particular and already pre-specified solution as presented by *Eqs. (A1)-(A11)* in Sadeghi *et al.* (2018), the far more general solution [†]

$$\left.\begin{aligned} &\xi_t = F_1(t), \\ &\xi_{x_2} = \mathcal{F}_2(t, x_2), \\ &\eta_{\overline{U}_1} = a_1 \overline{U}_1 - \overline{U}_1 \partial_{x_2}\mathcal{F}_2(t, x_2) + \mathcal{F}_3(t, x_2), \\ &\eta_{H^0_{12}} = a_1 H^0_{12} + \overline{U}_1 \partial_t \mathcal{F}_2(t, x_2) - H^0_{12}\partial_t F_1(t) + \mathcal{F}_4(t, x_2), \text{ where } \partial_{x_2}\mathcal{F}_4 = -\partial_t \mathcal{F}_3, \\ &\eta_{H^0_{ii}} = \overline{U}_1 \mathcal{F}_{5,i,1}(t, x_2) + H^0_{12}\mathcal{F}_{5,i,12}(t, x_2) + \textstyle\sum_{j=1}^{3} H^0_{jj}\mathcal{F}_{5,i,jj}(t, x_2) + \mathcal{F}_{5,i,0}(t, x_2), \end{aligned}\right\} \tag{2.4}$$

[†]To note is that the general solution (2.4) can also be derived from the 2-point correlation equations along with their continuity constraints as described in Sadeghi *et al.* (2018), by letting in the end the correlation length $\mathbf{r}$ in the solutions go to zero.

after exploiting the spanwise (x_3) symmetry of the flow configuration.[†] By augmenting the defining system (2.1) with the still required mass flux constraint $\int_{-\infty}^{\infty} \overline{U}_1 dx_2 = \text{const.}$, will restrict the general solution (2.4) only marginally to:

$$a_1 = 0, \quad \text{and} \quad \int_{-\infty}^{\infty} \mathcal{F}_3(t, x_2) dx_2 = 0, \tag{2.5}$$

i.e., $\mathcal{F}_3$ should be antisymmetric in x_2; the derivation of these two restrictions is given in Appendix A. For the sake of brevity, the solutions for the triple-velocity and pressure-velocity correlations are not shown here at this stage in (2.4); they will be shown further below when we try to consistently reduce the complexity of this solution. The presentation of (2.4) should only give a first impression of the high degree of arbitrariness which is involved here through the emergence of arbitrary space-time functions $\mathcal{F}$ for each variable.[‡] Also, it gives the correct impression of what from the outset a Lie-group invariance analysis can predict, without any prior intervention from the user: For a temporally evolving plane jet, as in (2.4), not too much, as the degree of arbitrariness is too high here in this case. In this sense, the presentation of the "general" equivalence solution given in Sadeghi *et al.* (2018) by *Eqs. (A1)-(A11)* is highly misleading, as the reader might think that this reduced solution is already the most general solution any Lie-group invariance analysis would give, particularly, as nowhere in the text it is mentioned that *Eqs. (A1)-(A11)* is actually only a reduced solution and that it thus, in fact, already constitutes a biased solution specified by the user.[‡‡]

This is exactly what will be done now, to reduce the immense complexity of the general equivalence solution (2.4) into a manageable expression. The guideline should be to conduct the reduction in a consistent and physically meaningful way. The first step should be to establish a connection to the classical scaling relations, since experimental and numerical evidence *approximately* support this scaling for the mean velocity field $\overline{U}_1$ as well as for the off-diagonal Reynolds stress R^0_{12}. The classical invariant scalings for these two fields are (see Sadeghi *et al.* (2018) for details)

$$\tilde{\overline{U}}_1(\tilde{x}_2) = \frac{\overline{U}_1(t, x_2)}{U_c(t)}, \qquad \tilde{R}^0_{12}(\tilde{x}_2) = \frac{R^0_{12}(t, x_2)}{U_c^2(t)}, \tag{2.6}$$

where $\tilde{\overline{U}}_1$ and $\tilde{R}^0_{12}$ are the corresponding self-similar fields, defined as a function of the similarity variable

$$\tilde{x}_2 = \frac{x_2}{\delta_{0.5}(t)}, \quad \text{with the jet half-width:} \quad \delta_{0.5}(t) = B\sqrt{t - t_0}, \tag{2.7}$$

being the dimensionless invariant lateral distance, and normalized by the mean velocity on the centreline ($x_2 = 0$)

$$\overline{U}_1(t, 0) =: U_c(t) = \frac{A}{\sqrt{t - t_0}}. \tag{2.8}$$

For an initial Reynolds number of 8000, based on the initial centreline velocity $U_c(0)$ and the initial jet thickness $\delta_{0.5}(0)$, the global constants A, B and t_0 were numerically best fitted in Sadeghi *et al.* (2018) to the values

$$A = 1.91, \qquad B = 1/A = 0.524, \qquad t_0 = 8.64, \tag{2.9}$$

in the time range $20 \leq t \leq 30$, where A and B both carry the same dimension of $L/\sqrt{T}$.

Now, when looking at the self-similar profile of the mean velocity (see *Fig. 3* in Sadeghi *et al.* (2018)), it *approximately* reminds us of a Gaussian profile being the solution of the diffusion equation. And since, in particular, the dimensionless and self-similar scaling (2.7) and (2.6) is compatible with

[†]Due to spanwise homogeneity and a spanwise reflection symmetry in the flow, all moments involving an uneven number of spanwise velocity fields vanish.

[‡]Except for the infinitesimal equivalence generator of the time variable ξ_t, which is an arbitrary function only of time and not of space.

[‡‡]It is straightforward to see that when choosing in (2.4) the arbitrary space-time functions $\mathcal{F}$ appropriately, that it will reduce to the particular solution *Eqs. (A1)-(A7)* in Sadeghi *et al.* (2018). However, the generators for the triple-velocities $\eta_{H^0_{ij2}}$ *(Eqs. (A8)-(A9))* in Sadeghi *et al.* (2018) are not correct, as they all miss a term proportional to $H^0_{ij}\partial_t\xi_{x_2}$. Furthermore, *Eq. (A7)* contains a misprint: Instead of $F_3(t)\overline{U}_1$, this term should read $(\partial_t F_3(t))\overline{U}_1$.

the diffusion equation when re-scaled into an overall dimensionless form

$$\frac{\partial\left(\frac{\overline{U}_1}{A/\sqrt{T}}\right)}{\partial\left(\frac{t}{T}\right)}=\frac{\partial^2\left(\frac{\overline{U}_1}{A/\sqrt{T}}\right)}{\partial\left(\frac{x_2}{B\sqrt{T}}\right)^2}\qquad\Longleftrightarrow\qquad\frac{\partial\overline{U}_1}{\partial t}=\nu_T\frac{\partial^2\overline{U}_1}{\partial x_2^2},\ \text{ with }\ \nu_T=B^2=0.275,\tag{2.10}$$

where B^2 then can be identified as the turbulent viscosity ν_T, which here for a Reynolds-number of 8000 takes the specific value 0.275, it is thus, in a first approximative sense, physically reasonable and not far-fetched to augment, within the considered time range $20\leq t\leq 30$, the statistically unclosed system (2.1) with equation (2.10) as an *approximate* defining equation[†] for the mean velocity $\overline{U}_1$

$$\partial_t\overline{U}_1=\nu_T\partial_{x_2}^2\overline{U}_1,\tag{2.11}$$

but, and this is important, with a still unknown initial condition[‡] within $20\leq t\leq 30$.

Re-performing the Lie-group invariance analysis of system (2.1) by including equation (2.11), will restrict in (2.4) three arbitrary functions: The two functions for ξ_t and ξ_{x_2} down to two linearly uncoupled functions

$$F_1(t)=t-c_1,\qquad\mathcal{F}_2(t,x_2)=\tfrac{1}{2}(x_2-c_2),\tag{2.12}$$

where c_1 and c_2 are arbitrary constants, and the function $\mathcal{F}_3$ down to be a particular solution of the diffusion equation (2.11). The complete solution for the infinitesimal equivalence generators (2.4) thus then reads (including the restrictions (2.5))

$$\left.\begin{aligned}
&\xi_t=t-c_1,\\
&\xi_{x_2}=\tfrac{1}{2}(x_2-c_2),\\
&\eta_{\overline{U}_1}=-\tfrac{1}{2}\overline{U}_1+\mathcal{F}_3(t,x_2),\ \text{where}\ \ \partial_t\mathcal{F}_3=\nu_T\partial_{x_2}^2\mathcal{F}_3,\ \text{and}\ \ \textstyle\int_{-\infty}^{\infty}\mathcal{F}_3dx_2=0,\\
&\eta_{H^0_{12}}=-H^0_{12}+\mathcal{F}_4(t,x_2),\ \text{where}\ \ \partial_{x_2}\mathcal{F}_4=-\partial_t\mathcal{F}_3,\\
&\eta_{H^0_{ii}}=\overline{U}_1\mathcal{F}_{5,i,1}(t,x_2)+H^0_{12}\mathcal{F}_{5,i,12}(t,x_2)+\textstyle\sum_{j=1}^{3}H^0_{jj}\mathcal{F}_{5,i,jj}(t,x_2)+\mathcal{F}_{5,i,0}(t,x_2),\\
&\eta_{H^0_{122}}=-\tfrac{3}{2}H^0_{122}-\tfrac{3}{2}\overline{PU_1}^0-\eta_{\overline{PU_1}^0}+\mathcal{F}_6(t,x_2),\\
&\eta_{H^0_{ii2}}=-\tfrac{1}{2}H^0_{ii2}+H^0_{12}\mathcal{F}_{5,i,1}(t,x_2)+H^0_{122}\mathcal{F}_{5,i,12}(t,x_2)+\textstyle\sum_{j=1}^{3}H^0_{jj2}\mathcal{F}_{5,i,jj}(t,x_2)\\
&\qquad\quad+\overline{PU_1}^0\mathcal{F}_{5,i,12}(t,x_2)+2\overline{PU_2}^0\mathcal{F}_{5,i,22}(t,x_2)-\delta_{i2}\left(\overline{PU_2}^0+2\eta_{\overline{PU_2}^0}\right)+\mathcal{F}_{7,i,0}(t,x_2),\\
&\eta_{\overline{PU_1}^0}=\mathcal{F}_8(t,x_2,\overline{U}_1,H^0_{12},H^0_{ii},H^0_{122},H^0_{ii2},\overline{PU_1}^0,\overline{PU_2}^0,\Phi^0_{ij}),\\
&\eta_{\overline{PU_2}^0}=\mathcal{F}_9(t,x_2,\overline{U}_1,H^0_{12},H^0_{ii},H^0_{122},H^0_{ii2},\overline{PU_1}^0,\overline{PU_2}^0,\Phi^0_{ij}),
\end{aligned}\right\}\tag{2.13}$$

where $\mathcal{F}_8$ and $\mathcal{F}_9$ are fully arbitrary functions in all variables involved. For the sake of brevity, the lengthy expressions for the pressure-rate-of-strain generators $\eta_{\Phi^0_{ij}}$ are not shown here, in particular as they also do not reveal any exciting new information, since they basically just compensate the functional structures given by the above triple-velocity and pressure-velocity correlations.

Although the original and untouched equivalence solution (2.4) got drastically reduced in the independent variables when including the empirically consistent assumption (2.11) as a further constraint to the defining system (2.1), the resulting solution (2.13) is still highly arbitrary in all its dependent variables. In the next section, a specific choice for these unclosed terms will be made. Although a physically consistent choice is made, it is not dictated by theory. It is a purely empirical choice, to be only seen as a single particular choice within an infinite trial-and-error process of infinitely many other possible choices on a way to find the optimal choice that will match numerical or experimental data best.

[†]Later, in Sec. 4 a better and higher-order approximation will be given based on the finding by Bradbury (1965).

[‡]Although (2.11) as a Cauchy problem can be generally solved within the time range $20\leq t\leq 30$ as

$$\overline{U}_1(t,x_2)=\tfrac{1}{\sqrt{4\pi\nu_T(t-20)}}\textstyle\int_{-\infty}^{\infty}dx_2'\overline{U}_1(20,x_2')e^{-\frac{(x_2-x_2')^2}{4\nu_T(t-20)}},$$

a concrete solution can only be generated if the initial condition $\overline{U}_1(20,x_2)$ is priorly known or pre-established.

3. Specifying a particular equivalence solution

In the following, let the set of open constants and arbitrary functions in (2.13) up to second moment be specifically chosen as:

$$\left.\begin{aligned} &c_1 = t_0, \quad c_2 = 0, \quad \mathcal{F}_3 = \mathcal{F}_4 = \mathcal{F}_{5,i,1} = \mathcal{F}_{5,i,12} = 0, \quad \mathcal{F}_{5,i,jj} = -\delta_{ij}, \quad \forall i,j, \\ &\mathcal{F}_{5,i,0} = \frac{\alpha_i}{\sqrt{t-t_0}} e^{-\frac{\beta x_2^2}{t-t_0}}, \quad \mathcal{F}_8 = -\tfrac{3}{2}\overline{PU_1}^0 - \overline{U}_1 \mathcal{F}_{5,2,0} + \mathcal{G}_1, \quad \mathcal{F}_9 = -\tfrac{3}{2}\overline{PU_2}^0 + \mathcal{G}_2, \end{aligned}\right\} \tag{3.1}$$

where α_i and β are arbitrary constants, and $\mathcal{G}_1$ and $\mathcal{G}_2$ arbitrary functions of space and time only. The equivalence generators (2.13) then take the explicit form

$$\left.\begin{aligned} &\xi_t = t - t_0, \quad \xi_{x_2} = \tfrac{1}{2} x_2, \quad \eta_{\overline{U}_1} = -\tfrac{1}{2}\overline{U}_1, \\ &\eta_{H^0_{12}} = -H^0_{12}, \quad \eta_{H^0_{ii}} = -H^0_{ii} + \frac{\alpha_i}{\sqrt{t-t_0}} e^{-\frac{\beta x_2^2}{t-t_0}}, \\ &\eta_{H^0_{122}} = -\tfrac{3}{2} H^0_{122} + \overline{U}_1 \frac{\alpha_2}{\sqrt{t-t_0}} e^{-\frac{\beta x_2^2}{t-t_0}} - \mathcal{G}_1(t,x_2) + \mathcal{F}_6(t,x_2), \\ &\eta_{H^0_{ii2}} = -\tfrac{3}{2} H^0_{ii2} - 2\delta_{i2}\mathcal{G}_2(t,x_2) + \mathcal{F}_{7,i,0}(t,x_2), \\ &\eta_{\overline{PU_1}^0} = -\tfrac{3}{2}\overline{PU_1}^0 - \overline{U}_1 \frac{\alpha_2}{\sqrt{t-t_0}} e^{-\frac{\beta x_2^2}{t-t_0}} + \mathcal{G}_1(t,x_2), \\ &\eta_{\overline{PU_2}^0} = -\tfrac{3}{2}\overline{PU_2}^0 + \mathcal{G}_2(t,x_2), \end{aligned}\right\} \tag{3.2}$$

where, up to the four global constants α_i and β, the generators for the mean velocity $\overline{U}_1$ and the Reynolds stresses $R^0_{ij} = H^0_{ij} - \delta_{1i}\delta_{1j}\overline{U}_1^2$ (2.3) are fully specified now.

To note is that (3.1) is an empirical choice and not dictated by theory. It is only one particular choice among infinitely many other choices that, as we will see in the next section, will scale the numerical profiles for the mean velocity and the Reynolds stresses appropriately. Hence, other choices may exist 'out there' that will scale equally well or even better. The only theoretical guideline that was explicitly used for (3.1) was the classical principle of cause and effect (see e.g. Frewer *et al.* (2015, 2016) and Appendix A in Frewer *et al.* (2017) for theoretical details), to assure as a minimal requirement that the choice made in (3.1) is at least physically consistent.

Indeed, as shown in Appendix B, the above choice (3.2) is physically consistent in the sense that there exists at least a single cause on the instantaneous (fluctuating) level such that the set of transformations (3.2) can emerge as a collective invariance on the statistical level. This particular choice (3.2) stands in stark contrast to the choice made in Sadeghi *et al.* (2018), in particular the proposed triple-velocity transformation $\eta_{H^0_{122}}$*(Eq. (A8))* which, in relation to all preceding lower-order moment transformations *Eqs. (A1)-(A7)*, is unphysical, since no cause of any type and form on the fluctuating level exists such that this transformation can emerge as an invariance on the statistical level. In relation to the specified lower-order moments *Eqs. (A1)-(A7)*, the invariant transformation $\eta_{H^0_{122}}$ *(Eq. (A8))* would only be physically consistent if it would contain a term proportional to the mean velocity $\overline{U}_1$, but, which is not the case, even when adding the terms that are originally missing from this expression (see last footnote on p. 3).

Following the procedure as outlined in Sadeghi *et al.* (2018), the corresponding invariant variables of system (3.2) for the mean velocity and the Reynolds stresses, which would let collapse differently timed spatial profiles in the range $20 \leq t \leq 30$ into a single profile,[†] are generated by solving the

[†]Note that the collapsing of profiles can only occur approximately and not exactly. The aim of this whole endeavour is namely to find the best approximation, which again is directly related to find a physically consistent set of invariant transformations in (2.13) that does it best.

following invariant surface conditions

$$\left.\begin{gathered}\xi_t\partial_t\overline{U}_1+\xi_{x_2}\partial_{x_2}\overline{U}_1-\eta_{\overline{U}_1}=0,\\ \xi_t\partial_t H^0_{12}+\xi_{x_2}\partial_{x_2}H^0_{12}-\eta_{H^0_{12}}=0,\quad \xi_t\partial_t H^0_{ii}+\xi_{x_2}\partial_{x_2}H^0_{ii}-\eta_{H^0_{ii}}=0,\end{gathered}\right\}\tag{3.3}$$

in each dependent variable for the constant of integration, which, since we are dealing here with PDEs, will be arbitrary functions symbolized in the following by Ψ. Hence, when incorporating the definitions (2.7) and (2.8) into the general solutions of (3.3), the invariant variable for the mean velocity and for the off-diagonal Reynolds stress then take the explicit form

$$\left.\begin{aligned}\overline{U}_1(t,x_2)&=\frac{\Psi_1\left(\frac{x_2}{\sqrt{t-t_0}}\right)}{\sqrt{t-t_0}}\\ &\equiv\frac{A\widehat{\Psi}_1\left(\frac{x_2}{B\sqrt{t-t_0}}\right)}{\sqrt{t-t_0}}\quad\Longleftrightarrow\quad\tilde{\overline{U}}_1(\tilde{x}_2)=\frac{\overline{U}_1(t,x_2)}{U_c(t)},\\ H^0_{12}(t,x_2)=R^0_{12}(t,x_2)&=\frac{A^2\widehat{\Psi}_{12}\left(\frac{x_2}{B\sqrt{t-t_0}}\right)}{t-t_0}\quad\Longleftrightarrow\quad\tilde{R}^0_{12}(\tilde{x}_2)=\frac{R^0_{12}(t,x_2)}{U_c^2(t)},\end{aligned}\right\}\tag{3.4}$$

which correspond to the classical scaling (2.6), while the three diagonal or normal Reynolds stresses scale differently as

$$\begin{aligned}H^0_{ii}(t,x_2)=R^0_{ii}(t,x_2)+\delta_{i1}\overline{U}_1^2(t,x_2)&=\frac{2\alpha_i}{\sqrt{t-t_0}}e^{-\frac{\beta x_2^2}{t-t_0}}+\frac{A^2\widehat{\Psi}_{ii}\left(\frac{x_2}{B\sqrt{t-t_0}}\right)}{t-t_0}\\ \Longleftrightarrow\quad\tilde{R}^0_{ii}(\tilde{x}_2)&=\frac{R^0_{ii}(t,x_2)+\delta_{i1}\overline{U}_1^2(t,x_2)}{U_c^2(t)}-\frac{2\alpha_i\sqrt{t-t_0}}{A^2}e^{-\frac{\beta x_2^2}{t-t_0}}.\end{aligned}\tag{3.5}$$

4. Comparing the scaling performance to DNS

The numerical simulation to be compared to is taken from the DNS performed by Sadeghi *et al.* (2018). The relevant data presented in *Fig. 3* (p. 248) and *Fig. 4* (p. 249) have been extracted using the plot-digitizer software WebPlotDigitizer, and is represented again in Fig. 1 in order to explicitly contrast it to the original data given in Sadeghi *et al.* (2018). For each variable, only three data sets within the considered time range $20\leq t\leq 30$ have been extracted as it shows to be sufficient: The lower end at $t=20$ ($\square$), the mid-value at $t=25$ ($\triangle$), and the upper end at $t=30$ ($\circ$).

While in Fig. 1 the classical normalizations (3.4) for the mean velocity $\tilde{\overline{U}}_1(\tilde{x}_2)$ and the off-diagonal Reynolds stress $g_{12}(\tilde{x}_2)=R^0_{12}(t,x_2)/U_c^2(t)=\tilde{R}^0_{12}(\tilde{x}_2)$ already scale appropriately by showing a satisfactory global collapse for different times over the full invariant domain, this cannot be said for the three normal or diagonal Reynolds stresses which near the centre region of the jet ($x_2\sim\tilde{x}_2\sim 0$) deviate significantly from being self-similar when using the same classical normalization as for the off-diagonal component: $g_{ii}(\tilde{x}_2)=R^0_{ii}(t,x_2)/U_c^2(t)$ (Sadeghi *et al.*, 2018, p. 248).

Using, however, the non-classical renormalization (3.5) for the normal stresses by taking for the global parameters the best fitted values $\beta=\ln(2)/B^2$, $\alpha_1=-0.028$, $\alpha_2=-0.035$, $\alpha_3=-0.022$, all profiles for each stress then satisfactorily collapse into a single profile globally as shown in Fig. 2. Worthwhile to note here is that the fitting result $\beta=\ln 2/B^2$ turns the initial specification of $\mathcal{F}_{5,i,0}$ in (3.1) into a best-fit function for the mean velocity profile, but only up to its turning point around $\tilde{x}_2=\tilde{x}_2^0\sim 0.85$, i.e., within this range the mean velocity profile of a temporally evolving turbulent plane jet can be well approximated by

$$\overline{U}_1(t,x_2)=\frac{A}{\sqrt{t-t_0}}e^{-\frac{\ln 2\cdot x_2^2}{B^2(t-t_0)}},\quad\text{for}\quad\tilde{x}_2\leq\tilde{x}_2^0\sim 0.85,\tag{4.1}$$

but which for $B^2=\nu_T$, unfortunately, deviates from being a solution of the diffusion equation (2.11) by nearly a factor 3 in the exponent. Hence, the approximation initially made in Sec. 2, namely to

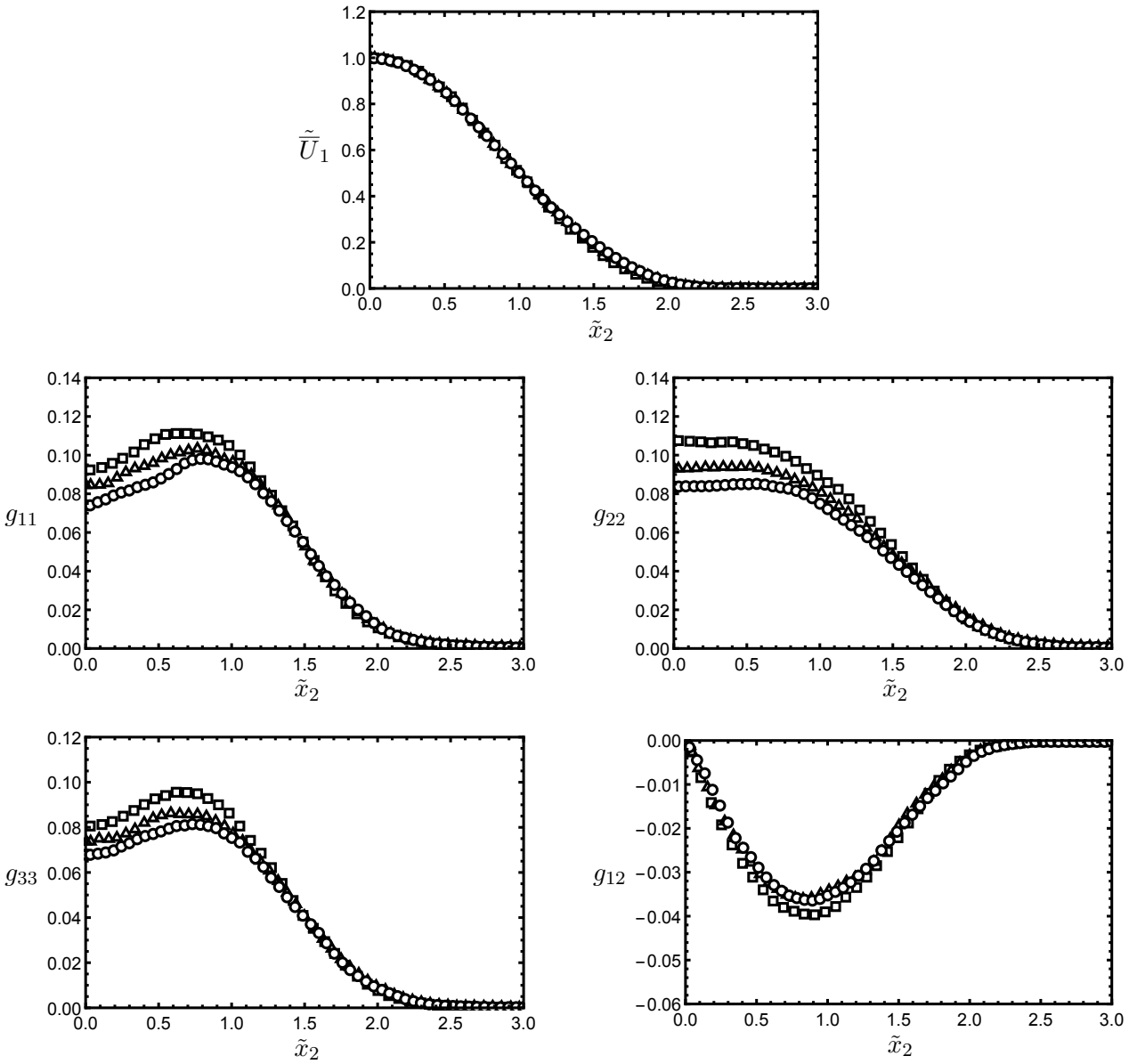

Figure 1: Extracted data sets from *Figs. 3-4* of Sadeghi *et al.* (2018) for $t = 20$ (□), $t = 25$ (△), and $t = 30$ (○). The axes labelling refer to the normalized variables: $\tilde{x}_2 = x_2/\delta_{0.5}(t)$ (2.7), $\widetilde{\overline{U}}_1(\tilde{x}_2) = \overline{U}_1(t, x_2)/U_c(t)$ (2.8), and $g_{ij}(\tilde{x}_2) = R^0_{ij}(t, x_2)/U_c(t)^2$ as defined on p. 248 in Sadeghi *et al.* (2018).

augment the unclosed set of statistical moment equations (2.1) with the diffusion equation (2.11) as a defining equation for the mean velocity $\overline{U}_1$, is a rather poor approximation. A better approximation can be generated by using the finding of Bradbury (1965)[†], namely to model the mean velocity in its invariant variable to higher order as

$$\overline{U}_1(t, x_2) = \frac{A}{\sqrt{t - t_0}} e^{-\frac{\ln 2 \cdot x_2^2}{B^2(t-t_0)} - \frac{\gamma \cdot x_2^6}{B^6(t-t_0)^3}}, \tag{4.2}$$

which then offers a satisfactory approximation in the whole invariant domain $\tilde{x}_2 = x_2/\delta_{0.5}(t)$ (2.7). A best fit to the data shown in Fig. 1 will fix the higher order exponent to $\gamma = 0.024 \cdot \ln 2$, which, not surprisingly, corresponds more or less to the value proposed in Bradbury (1965).

The aim now is to associate the function (4.2) to a certain transport equation that will replace the initial approximation (2.11) by a better one, however, such that the classical scaling for the mean

[†]Note that Bradbury (1965) considered a spatially evolving jet flow, yet the self-similar result for the mean velocity can be transcribed to a temporally evolving flow just by switching the dimensionless invariant variable from $x_2/\delta_{0.5}(x_1)$ to $x_2/\delta_{0.5}(t)$ — see also the introductory discussion in Sadeghi *et al.* (2018).

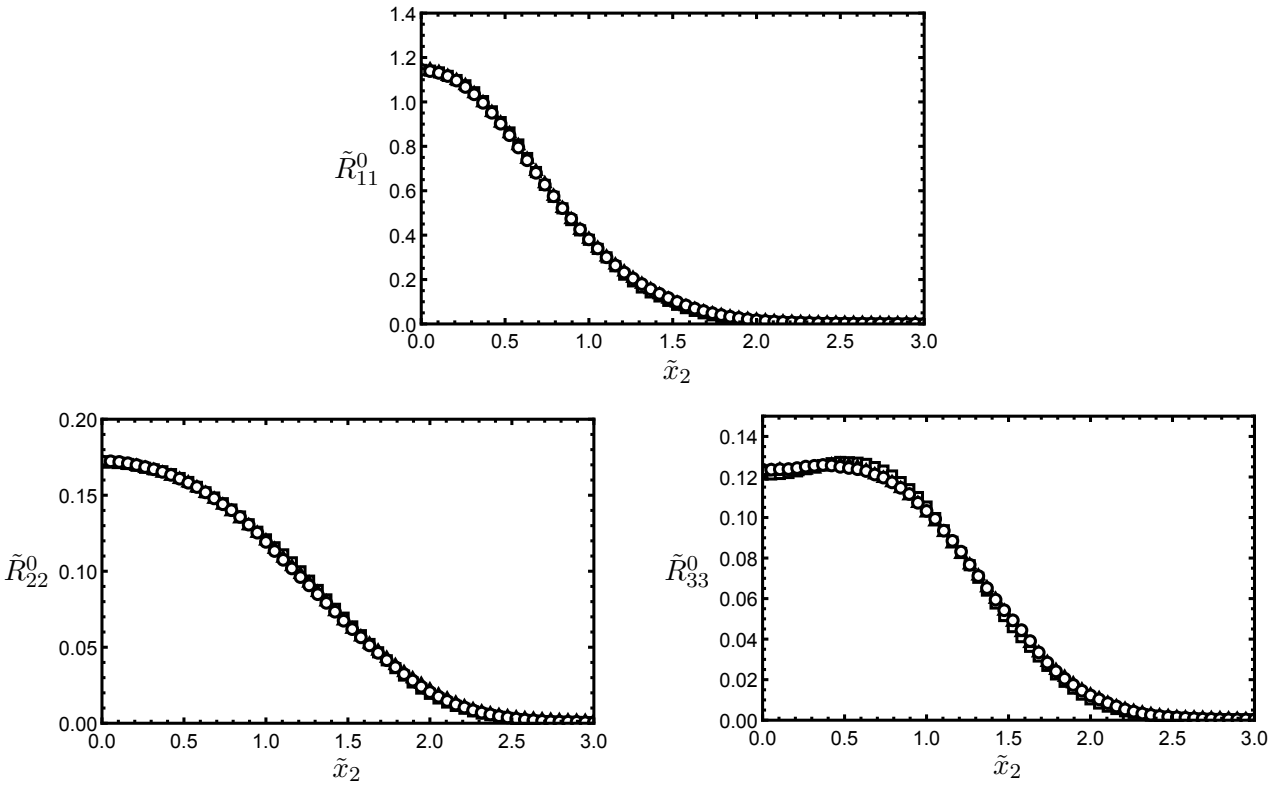

Figure 2: Renormalized diagonal Reynolds stresses according to (3.5). In contrast to the classical normalization shown in Fig. 1, a global self-similar behaviour can now be observed extending over the full invariant domain $\tilde{x}_2$. Within a best fit, the four global parameters in (3.5) were fixed to: $\beta = \ln(2)/B^2$, $\alpha_1 = -0.028$, $\alpha_2 = -0.035$, and $\alpha_3 = -0.022$. As in Fig. 1, the above symbols refer again to: $t = 20$ ($\square$), $t = 25$ ($\triangle$), and $t = 30$ ($\circ$).

velocity (2.6) is not destroyed. In other words, the aim is to augment again the unclosed set of statistical moment equations (2.1) with a defining equation for the mean velocity, but now with a better, higher-order approximate equation than the one initially proposed by (2.11); but, also such that the infinitesimal equivalence generators for ξ_t, ξ_{x_2} and $\eta_{\overline{U}_1}$, as generally given by (2.4), can reduce to those of (3.2) when performing again a Lie-group invariance analysis on this new combined system. Now, since the function (4.2) can be seen as a particular solution of the following modified (non-autonomous) diffusion equation

$$\partial_t \overline{U}_1 = B^2 \partial^2_{x_2} \overline{U}_1 + \frac{\overline{U}_1}{t - t_0} \sum_{n=1}^{6} \mu_n \left(\frac{x_2}{B\sqrt{t - t_0}} \right)^{2n-2}, \tag{4.3}$$

where the dimensionless parameters take on the values

$$\left.\begin{array}{lll} \mu_1 = 2\ln 2 - \frac{1}{2}, & \mu_2 = \ln 2 \cdot (1 - 4\ln 2), & \mu_3 = 30\gamma, \\ \mu_4 = \gamma \cdot (3 - 24\ln 2), & \mu_5 = 0, & \mu_6 = -36\gamma^2, \end{array}\right\} \tag{4.4}$$

and since this equation meets all requirements mentioned above, (4.3) is an appropriate higher-order approximation to (2.11). Indeed, when re-performing a full Lie-group invariance analysis on the defining but unclosed system (2.1) augmented with (4.3) and restricted by the mass flux constraint (2.5), we will obtain the same general result (2.13) as before, except that c_1, c_2 and $\mathcal{F}_3$ are now specifically restricted to

$$c_1 = t_0, \quad c_2 = 0, \quad \partial_t \mathcal{F}_3 = B^2 \partial^2_{x_2} \mathcal{F}_3 + \frac{\mathcal{F}_3}{t - t_0} \sum_{n=1}^{6} \mu_n \left(\frac{x_2}{B\sqrt{t - t_0}} \right)^{2n-2} \text{ and } \int_{-\infty}^{\infty} \mathcal{F}_3 dx_2 = 0. \tag{4.5}$$

This allows us now to make the specific higher-order choice for $\mathcal{F}_{5,i,0}$ in (3.1) as

$$\mathcal{F}_{5,i,0} = \frac{\hat{\alpha}_i}{\sqrt{t - t_0}} e^{-\frac{\ln 2 \cdot x_2^2}{B^2(t-t_0)} - \frac{\gamma \cdot x_2^6}{B^6 (t-t_0)^3}}, \quad \gamma = 0.024 \cdot \ln 2, \tag{4.6}$$

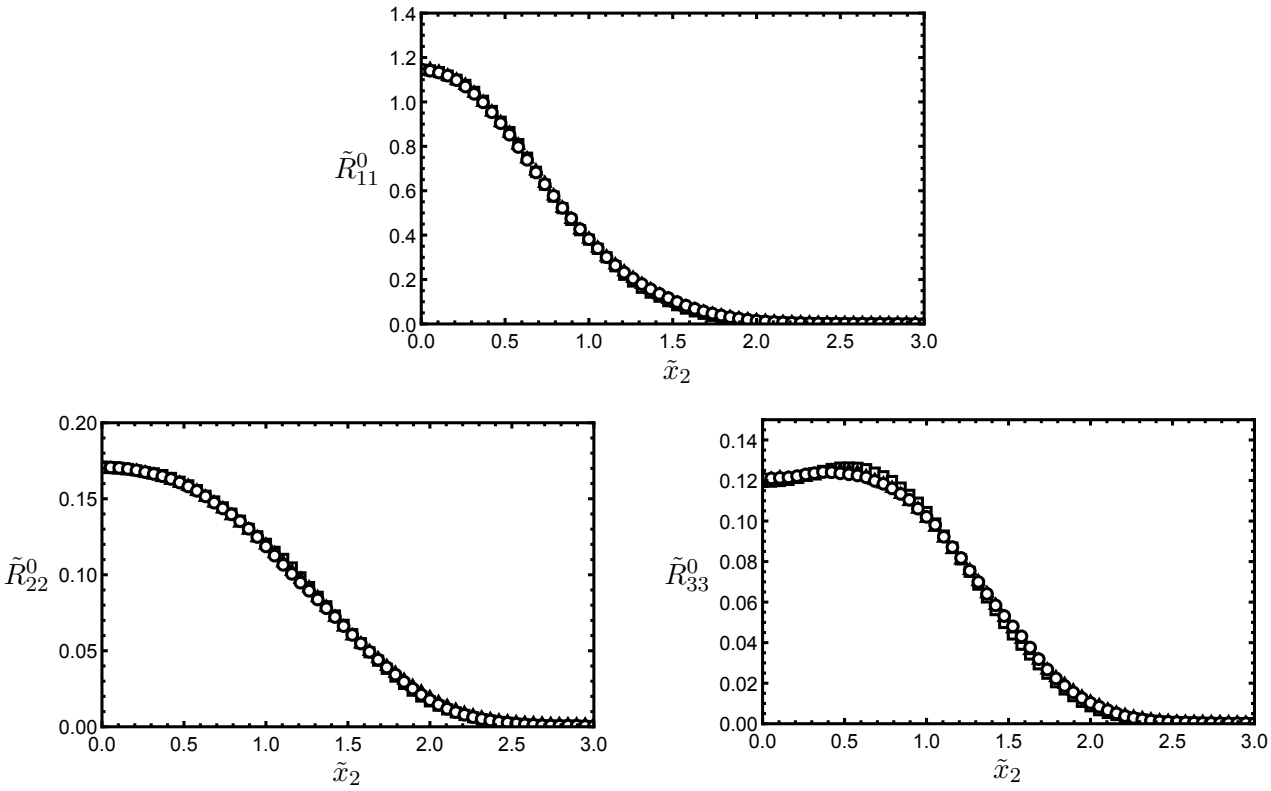

Figure 3: Renormalized diagonal Reynolds stresses according to the higher-order approximation (4.9). However, when comparing to the former scaling shown in Fig. 2, no improvement can be registered. As discussed in the text, maybe this improvement only will become visible when also considering the appropriate scaling for higher-order moments beyond the Reynolds stresses. Within a best fit, the three global parameters in (4.9) were fixed to: $\hat{\alpha}'_1 = -0.015$, $\hat{\alpha}'_2 = -0.018$, and $\hat{\alpha}'_3 = -0.011$. As in Fig. 2, the above symbols again refer to: $t = 20$ (□), $t = 25$ (△), and $t = 30$ (○).

which now can be identified as a best-fit function proportional to the mean velocity field, that is, (4.6) can thus be well approximated by (4.2) as

$$\mathcal{F}_{5,i,0} = \hat{\alpha}'_i \, \overline{U}_1, \quad \text{where} \quad \hat{\alpha}'_i = \hat{\alpha}_i / A. \tag{4.7}$$

With this ansatz in (3.1), the equivalence generators (2.13) then take the explicit form

$$\left.\begin{aligned}
&\xi_t = t - t_0, \quad \xi_{x_2} = \tfrac{1}{2} x_2, \quad \eta_{\overline{U}_1} = -\tfrac{1}{2}\overline{U}_1, \\
&\eta_{H^0_{12}} = -H^0_{12}, \quad \eta_{H^0_{ii}} = -H^0_{ii} + \hat{\alpha}'_i \, \overline{U}_1, \\
&\eta_{H^0_{122}} = -\tfrac{3}{2} H^0_{122} + \hat{\alpha}'_2 \, \overline{U}_1^2 - \mathcal{G}_1(t, x_2) + \mathcal{F}_6(t, x_2), \\
&\eta_{H^0_{ii2}} = -\tfrac{3}{2} H^0_{ii2} - 2\delta_{i2} \mathcal{G}_2(t, x_2) + \mathcal{F}_{7,i,0}(t, x_2), \\
&\eta_{\overline{PU_1}^0} = -\tfrac{3}{2} \overline{PU_1}^0 - \hat{\alpha}'_2 \, \overline{U}_1 + \mathcal{G}_1(t, x_2), \\
&\eta_{\overline{PU_2}^0} = -\tfrac{3}{2} \overline{PU_2}^0 + \mathcal{G}_2(t, x_2),
\end{aligned}\right\} \tag{4.8}$$

which now can be seen as a higher-order approximation to the former equivalence solution (3.2). Solving for (4.8) the associated invariant surface conditions (3.3), the invariant variables for the mean velocity and Reynolds stresses then read

$$\tilde{\overline{U}}_1(\tilde{x}_2) = \frac{\overline{U}_1(t, x_2)}{U_c(t)}, \qquad \tilde{R}^0_{12}(\tilde{x}_2) = \frac{R^0_{12}(t, x_2)}{U_c^2(t)}, \qquad \tilde{R}^0_{ii}(\tilde{x}_2) = \frac{R^0_{ii}(t, x_2) + \delta_{i1} \overline{U}_1^2(t, x_2) - 2\hat{\alpha}'_i \, \overline{U}_1}{U_c^2(t)}. \tag{4.9}$$

By construction the scaling for the mean velocity and the off-diagonal Reynolds stress stay unchanged and are shown in Fig. 1. Different is only the scaling ansatz for the normal Reynolds stresses, which for $\hat{\alpha}'_1 = -0.015$, $\hat{\alpha}'_2 = -0.018$ and $\hat{\alpha}'_3 = -0.011$ is shown as a best fit in Fig. 3. However, when comparing to the former scaling shown in Fig. 2, no improvement can be registered. Hence, it seems that the improvement maybe only becomes visible when considering the scaling of higher-order moments beyond the Reynolds stresses as for the triple-velocities H^0_{ij2} — but for these we have no prior theoretical guarantee that the initial choice (3.1) made for the second moments is also consistent to any higher-order moment; maybe a different choice has to be made when including and studying the scaling behaviour of higher-order moments beyond the Reynolds stresses.

To close this section and in order to pass over to the next section, it is worth noting that when comparing Fig. 2, or Fig. 3, with the corresponding *Fig. 7* in Sadeghi *et al.* (2018), it seems at first sight that in both cases a similar result is obtained, although by *Eqs. (4.10)-(4.12)* in Sadeghi *et al.* (2018) a fundamentally different set of scaling relations for the normal Reynolds stresses is used than the one derived herein, either given by (3.5) or by (4.9). It seems that a key difference lies in the absolute value where the profiles collapse at $\tilde{x}_2 = 0$, but even this difference levels out when considering relative values: The ratios $\tilde{R}^0_{ii}(0)/\tilde{R}^0_{jj}(0)$ from Fig. 2, or Fig 3, equal more or less those from *Fig. 7* in Sadeghi *et al.* (2018). Despite all this resemblance between these figures, a key problem remains: *Fig. 7* in Sadeghi *et al.* (2018) cannot be reproduced. Their defining scaling relations *Eqs. (4.10)-(4.12)* for *Fig. 7* do not match to what is shown then in *Fig. 7*.

This mismatch can be easily seen just by looking at the asymptotic behaviour of the scaling relations *Eqs. (4.10)-(4.12)* for large x_2, or equivalently for large $\tilde{x}_2 = x_2/(B\sqrt{t - t_0})$ at some fixed finite value $t > t_0$, and then compare it to the asymptotic behaviour shown in *Fig. 7*: While all self-similar solutions in *Fig. 7* tend to zero, the corresponding self-similar solutions given by *Eqs. (4.10)-(4.12)* do not! Instead, for each field they tend to the finite value $a_{H_{ii}}t$, because in free planar jet flow all fields decay to zero for large lateral distances x_2 with the result that the field-proportional terms on the right-hand side of *Eqs. (4.10)-(4.12)* are thus negligible compared to the field-free terms $a_{H_{ii}}t$, which survive this limit.[†] Also, the values of these terms $a_{H_{ii}}t$[‡], first of all, are not small when compared to the maximum value of each profile for $t \geq 20$, and secondly tend to a different value for each different t, i.e., the self-similarity in the asymptotic region is lost due to the presence of these terms. Fig. 4 shows the correct corresponding plots for the scaling relations *Eqs. (4.10)-(4.12)* proposed in Sadeghi *et al.* (2018), clearly demonstrating the difference to what is shown in *Fig. 7* — to note is that at $\tilde{x}_2 = 0$ the plots for the normal Reynolds stresses in Fig. 4 exactly coincide in value with the corresponding plots in *Fig. 7*, thus corroborating that no mistake in Fig. 4 has been made. Fig. 4 also includes the similarity profile for the off-diagonal Reynolds stress R^0_{12}, which should scale as *Eq. (B5)* and shown in Sadeghi *et al.* (2018) by *Fig. 6*. Also this figure cannot be reproduced, since in comparison with the correct plot shown in Fig. 4 it is off by a global scaling factor of nearly 3: The correct maximum value for $\tilde{R}^0_{12}$ is nearly three times higher than shown in *Fig. 6*.

The reason for why the asymptotic self-similarity gets broken by *Eqs. (4.10)-(4.12)* is that this scaling is in fact based on an unphysical set of equivalence transformations, namely the choice *Eqs. (A4)-(A11)* made in Sadeghi *et al.* (2018) violates the classical principle of cause and effect, in the sense that there exists no cause on the instantaneous (fluctuating) level of the Navier-Stokes equations such that these equivalences can emerge as an effect on the statistical level. In other words, the equivalences *Eqs. (A4)-(A11)* put forward in Sadeghi *et al.* (2018) have no physical justification, they even violate the underlying physical principles. This claim is proven at the end of Appendix B. It stands in stark contrast to the equivalence transformations proposed in this comment, either given by (3.2) or by (4.8), which both do not violate the causality principle.

[†]Note that D given in *Eqs. (4.10)-(4.12)* in Sadeghi *et al.* (2018) is a constant and not some functional, taking the global value $D = -7.57$ (p. 249).

[‡]Taken from *Tab. 1* in Sadeghi *et al.* (2018), the globally constant and fixed values of $a_{H_{ii}}$ are: $a_{H_{11}} = 0.0383$, $a_{H_{22}} = 0.0706$, and $a_{H_{33}} = 0.0453$.

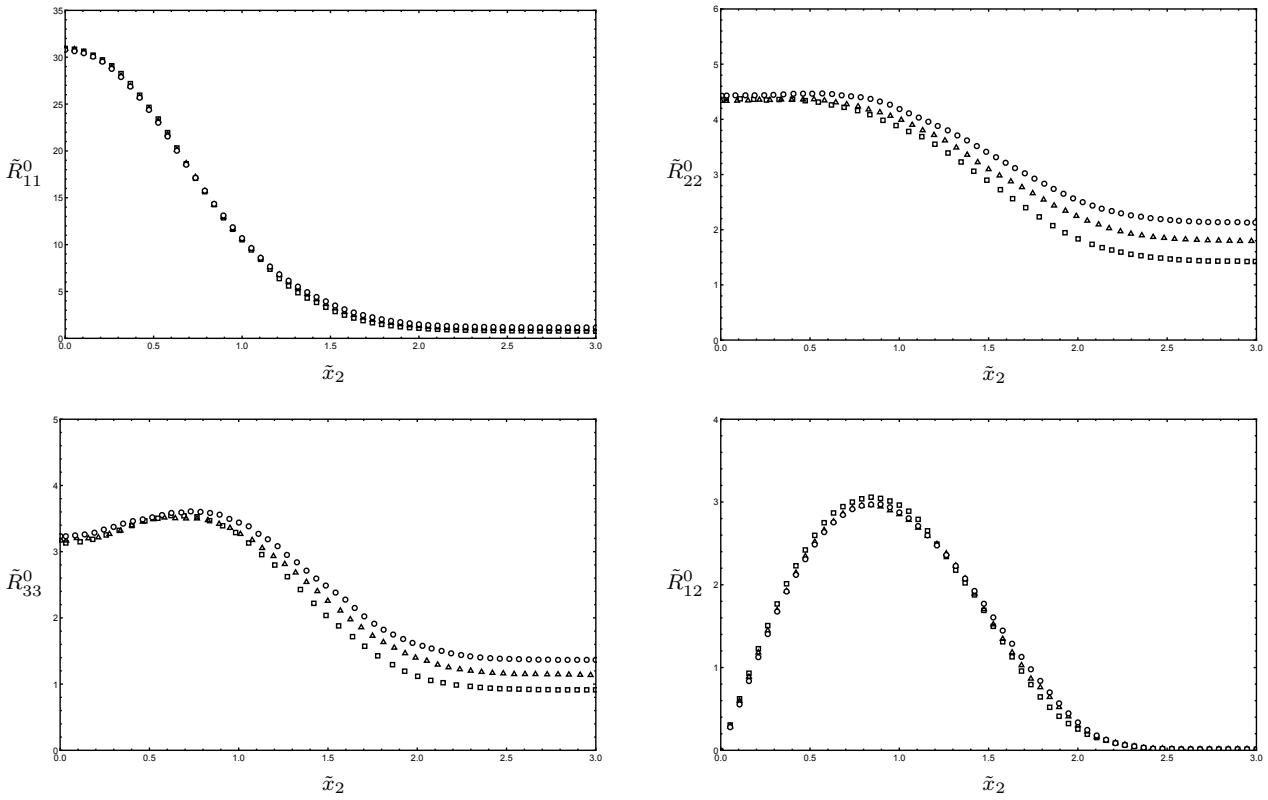

Figure 4: The correct plots associated to the self-similar scaling proposed in Sadeghi *et al.* (2018) by *Eqs. (4.10)-(4.12)* for the normal Reynolds stresses and by *Eq. (B5)* for the off-diagonal Reynolds stress. There is a clear discrepancy to the corresponding plots *(Figs. 6-7)* shown in Sadeghi *et al.* (2018). In contrast to *Fig. 7*, the normal Reynolds stresses do not tend to zero and do not collapse into a single profile for large invariant distances $\tilde{x}_2$. In other words, the above plots for the three normal Reynolds stresses do not show a self-similar behaviour for large $\tilde{x}_2$, as incorrectly claimed in Sadeghi *et al.* (2018). To note is that at $\tilde{x}_2 = 0$ the above plots for the normal Reynolds stresses exactly coincide in value with the corresponding plots in *Fig. 7*, thus corroborating that no mistake in the above plots have been made. Regarding the above lower right plot for the off-diagonal Reynolds stress, this correct profile is globally in scale nearly 3 times larger than the corresponding one shown in *Fig. 6*. For more details about this overall discrepancy, please see the text in Sec. 4 & 5. As in all figures before, the above symbols refer again to: $t = 20$ (□), $t = 25$ (△), and $t = 30$ (○).

5. A critical examination of Sadeghi *et al.* (2018): Refuting the study's claims

This section lists all (major and minor) problems to be found in Sadeghi *et al.* (2018), including two severe flaws (the first two listed below), which ultimately refutes the study as a whole:

(1): The interpretations and conclusions in that study are not justified by the results given. Particularly, *Fig. 7* cannot be reproduced from the given DNS data shown in *Fig. 4(a-c)* as claimed. The analytic asymptotic behaviours of the underlying *Eqs. (4.10)-(4.12)* do not match the corresponding numerical asymptotic behaviours as shown in *Fig. 7*: Firstly, when proposing a scaling as given by *Eqs. (4.10)-(4.12)*, a collapse of the profiles for large $\tilde{x}_2$ cannot be confirmed and, secondly, in this regime the profiles also do not tend to zero as incorrectly shown in *Fig. 7*.

That the profiles for the invariantized diagonal Reynolds stresses do not collapse and do not tend to zero in the asymptotic regime when scaled as *Eqs. (4.10)-(4.12)* can be easily seen by considering e.g. the case $\tilde{R}^0_{22}$ *(4.11)* — the reasoning for the other two cases *(4.10)* and *(4.12)* is analogous: Since in free planar jet flow all fields, including R^0_{22}, decay for large lateral distances x_2 and therefore also for large invariant distances $\tilde{x}_2 \propto x_2/\sqrt{t - t_0}$ *(Eqs. (3.6),(4.8)-(4.9))* for any fixed finite time t, say $t = 20$, the first term $-D \cdot R^0_{22} \cdot (t - t_0)$ on the right-hand side of *Eq. (4.11)* tends to zero.[†] Now, since this first term is negligibly small compared to the second one on the right-hand side $a_{H_{22}} t$, which, according to *Tab. 1* (p. 252) takes for $t = 20$ the finite and non-zero value $a_{H_{22}} t = 0.0706 \cdot 20 \sim 1.4$,

[†]As already noted before, D and t_0 in *Eqs. (4.10)-(4.12)* are empirically fixed constants, taking the global values $D = -7.57$ (p. 249) and $t_0 = 8.64$ (p. 247).

the asymptotic value for the invariantized Reynolds stress $\tilde{R}^0_{22}$ does not tend to zero, as incorrectly shown in *Fig. 7(b)*, but rather tends to the value 1.4. This is true also for any other profile, say $t = 30$, which would tend to the even higher value $a_{H_{22}}t = 0.0706 \cdot 30 \sim 2.1$, being even a different value than for the profile $t = 20$. Hence, for large $\tilde{x}_2$ the profiles for different t do not only go to a non-zero value but also do not collapse. Fig. 4 in this comment shows the correct profiles to the scaling proposed by Sadeghi *et al.* (2018). The discrepancy to their *Fig. 7* is clearly visible.

(2): The reason for this failure described above is that in that study again, as also already in all previous studies from the group of Oberlack *et al.*, unphysical statistical symmetries[†] are being employed that violate the classical principle of cause and effect. If the statistical symmetries of the system are chosen as given in *Appx. A* (p. 254), then, for example, the translation group $a_{H_{22}}$ of the double-velocity moment in *Eq. (A5)* is inconsistent to the symmetry for the triple-velocity moment H^0_{122} as given in *Eq. (A8)* or *Eq. (A9)*, which, in order to be consistent with the lower moment, needs to contain a term that is at least proportional to the mean velocity $\overline{U}_1$. See (3.2) or (4.8) in this comment for a choice of symmetries that do not violate the causality principle and which lead to a more convincing and robust collapsing of all profiles up to second order, as shown here in Fig. 2 and Fig. 3, respectively. The consistency proof is given in Appendix B.

(3): The result of their performed Lie-group symmetry analysis, as presented in *Eqs. (A1)-(A11)*, not only contains inaccuracies,[‡] but their analysis is also spectacularly incomplete. Irrespective of whether performing a 1-point symmetry analysis, or a more general 2-point symmetry analysis within the 1-point limit, in both cases, when done properly and correctly, will give an infinitely larger symmetry group than the one presented in *Appx. A* (p. 254), not only for all dependent variables but also for the independent variable x_2: Any correctly performed symmetry analysis for the inviscid ($\nu = 0$) free planar jet flow case will not lead to the linear x_2-specification from the outset as given in *Eq. (A2)*, but rather to an arbitrary function in x_2 and t, given in this comment by (2.4). Even when including the lateral mass flux constraint *Eq. (2.4)*, the symmetry generator ξ_{x_2} stays arbitrary and will not be restricted in a certain way — the mass flux constraint *Eq. (2.4)*, also in its original form $\int_{-\infty}^{\infty} \partial_t \overline{U}_1 dx_2 = 0$, only restricts the symmetry of the mean velocity $\overline{U}_1$ and not that of x_2, since all the restricting terms for x_2 will cancel exactly (after partial integration) — see Appendix A.

Of course, it is clear that one aims to make a connection to the classical x_2-invariant scaling $\tilde{x}_2 \propto x_2/\sqrt{t - t_0}$ and that for this very reason one has to choose a linear ansatz for the symmetry generator of x_2, but this particular choice is not given as an explicit result from Lie-group analysis itself. In other words, this particular choice is not given by theory from within, as misleadingly claimed in Sadeghi *et al.* (2018); instead it is put as an external condition to match the collapsing DNS profiles of the mean velocity field. The same is true for all other variables, except for ξ_t *(Eq. (A1))* which from the outset is already in its general form.

Hence, presenting the symmetry result in the reduced form as given in *Eqs. (A1)-(A11)* is misleading, as the reader might think that a Lie-group symmetry analysis for the inviscid free planar jet will only lead to this particular result *Eqs. (A1)-(A11)* without any further intervention by the user. But this is not the case: A consistent and complete symmetry analysis gives a highly arbitrary result, which, if one aims to match with experimental or numerical data, needs to be arranged and specified externally. Due to this arbitrariness in the symmetries, all derived scalings in that study (irrespective of their higher-order inconsistencies as described in ***(1)*** and ***(2)*** above) are thus only *a posteriori* scalings and not *a priori* scalings as wanted. Under such conditions as given in the theory of turbulence, a systematic Lie-group analysis cannot make and give any analytical prediction as to how turbulence scales statistically, due to that not only unknown parameters but also an abundance of arbitrary functions get induced. As convincingly shown in this comment, a collapse of all profiles can also be obtained when choosing a different set of symmetries than the one incorrectly proposed in Sadeghi *et al.* (2018), i.e., when choosing any set of symmetries which does not violate the classical principle of cause and effect. There is no prediction or no unique choice in the scaling as how to

[†]To keep in line with the (misleading) notation in Sadeghi *et al.* (2018), we will call all equivalences in this section as symmetries. As discussed and explained in Sec. 1, such an identification is misleading here, since all results derived and presented in Sadeghi *et al.* (2018) refer only to equivalence and not to symmetry transformations.

[‡]For example, if the symmetries for the double-velocity moments are chosen as given by *Eqs. (A4)-(A7)*, then the symmetry of each triple-velocity moment H^0_{ij2} misses the vital term proportional to H^0_{ij}. See also last footnote on p. 3.

make the profiles collapse; any other choice of symmetries with a cause will also do the job. Hence, it is *incorrect* to state that "within the present work, we develop a theoretical basis using a Lie symmetry group that predicts such behaviour for the flow evolution, as an exact solution of the two- and multi-point correlation equations, which can be an important key in 'filling the gaps' of our understanding of self-similarity" (p. 251). Instead of theoretically predicting flow evolution, Sadeghi *et al.* (2018) only presents and proposes a sophisticated post-processing scheme. Nothing more!

The real problem simply is that the underlying statistical transport equations are unclosed, and so are their symmetries. The closure problem of turbulence cannot be circumvented by just employing the method of Lie-group symmetry analysis alone. Hence, without modelling these unclosed equations, an *a priori* prediction as how turbulence scales is and will not be possible. Only *a posteriori*, by anticipating what to expect from numerical or experimental data, the adequate invariant scalings can be generated through an iterative trial-and-error process.

(4): For the above reason mentioned in beginning of ***(3)***, namely in presenting an incomplete symmetry analysis, it seems that the 1-point limit $\mathbf{r} \to 0$ in their symmetry analysis was not done correctly, thus leading to that overly restricted symmetry group. An indication for it is given on p. 242, when saying "we currently devote ourselves only to generating invariant scaling laws for the mean velocity and Reynolds stresses, and therefore, the r-dependency of the terms is skipped". Doing the 1-point limit, the r-dependency may not be simply dropped, as this may lead to missing terms. The problem here is that when performing the 1-point limit one has to respect the non-commutivity of this limit: For example $\lim_{\mathbf{x}_{(2)}\to\mathbf{x}_{(1)}} \partial_{\mathbf{x}_{(1)}} \overline{U_i(\mathbf{x}_{(1)})U_j(\mathbf{x}_{(2)})}$ is simply not just $\partial_{\mathbf{x}_{(1)}} \overline{U_i(\mathbf{x}_{(1)})U_j(\mathbf{x}_{(1)})}$; it is more than that if one chooses this particular form — for a detailed explanation, see e.g. *Eq. (C.27)* on p. 40 in Frewer *et al.* (2014*b*).

(5): The derivation of the invariant scaling *Eq. (B3)* from *Eq. (B2)* and *Eq. (B1)* is a deception. The first step to *(B1)* is that $\overline{U}_1 x_2$ is being identified as the invariant integration constant $\tilde{U}_1\tilde{x}_2$ in order to reduce the integration effort of equation *(B1)*. This step is correct and not to complain about. However, this constant $\tilde{U}_1\tilde{x}_2$ is also multiplied by the factor $dF_2(t)/dt$, which from the calibration done in *Sec. 4* has to be zero, since $F_2(t)$ is fixed as the global constant $F_2(t) = -Dn$ *(Eq. (4.9))*, i.e., $dF_2(t)/dt = 0$. This results into an equation *(B1)* which does not contain the term involving $\tilde{U}_1\tilde{x}_2$, and thus when integrated to *(B2)* should not contain this term either, because it is zero. Nevertheless, this term appears as an overall non-zero constant in *(B2)*, because $F_2(t) = -Dn$ is a non-zero constant. To solve this contradiction such that the integrated solution *(B2)* is consistent with its underlying equation *(B1)*, which again does not contain the term involving $\tilde{U}_1\tilde{x}_2$, this term appearing on the right-hand side of *(B2)* has to be transported and to be absorbed into the invariant tilde-expression on the left-hand side of *(B2)*, which is the collection pool of all integration constants. But definitely not as done in *(B3)*, by re-identifying the invariant constant $\tilde{U}_1\tilde{x}_2$ back to the non-invariant expression $\overline{U}_1 x_2$ and then by rewriting the factor $F_2(t)$ as an expression of $F_1(t)$ using relation *Eq. (3.11)*. Hence, the derivation of *(B3)* is not mathematically sound since the round-bracketed term on the right-hand side actually belongs on the left-hand side of *(B3)*. In fact, when comparing the classical scaling in *Fig. 4(d)* with the corresponding new scaling in *Fig. 6* described by *(B3)*, no improvement can be seen. Instead, the new scaling for the Reynolds stress R^0_{12} is rather weaker than the classical scaling, since next to the already exiting problematic region around $\tilde{x}_2 = 1$, a new problematic region around $\tilde{x}_2 = 1.5$ is induced which does not arise in classical scaling.

Besides this issue, it is further to note that also the plot for this newly scaled Reynolds stress $\tilde{R}^0_{12}$ as shown in *Fig. 6* cannot be fully reproduced too. It is off by a global scaling factor of nearly 3. The correct plot for $\tilde{R}^0_{12}$ according to the scaling by Sadeghi *et al.* (2018) is shown here in Fig. 4, revealing that the maximum value for $\tilde{R}^0_{12}$ is nearly three times higher than shown in *Fig. 6*.

(6): The title chosen for that study is misleading. Nowhere throughout that study any scaling *laws* are derived. Instead, scaling relations are derived with the aim to let numerical profiles of a certain field variable collapse. The functional structure of these collapsing profiles, however, remain unknown. Thus no prediction on the scaling behaviour of the statistical solutions is made, as incorrectly claimed on p. 251 and already discussed above in ***(3)***. For example, when integrating the invariant surface condition for the mean velocity profile, i.e., when integrating the first three terms of *Eq. (3.1)*, the solution will be an arbitrary function in terms of an arbitrary invariant variable involving next to x_2 the arbitrary temporal functions F_1, F_2 and F_3. And knowing from the result (2.4) in this comment,

that the invariant surface condition *Eq. (3.1)* is only a specification and not in its most general form, the arbitrariness in the set of invariant solutions is even higher from the outset than given by *Eq. (3.1)*. To obtain invariant scaling *laws*, a systematic Lie-group symmetry analysis is not of much help here, since it just shifts the arbitrariness from one function to another. For a further discussion of this point, see e.g. Frewer *et al.* (2014*a*); Frewer & Khujadze (2016).

(7): *Update, 5. Dec. 2018:* The criticism that was placed here in the earlier version (4. Oct. 2018), regarding a mislabelling of the horizontal axes for the plots in *Figs. 5-7*, was not justified. Because, when interpreting their small indication "$\tilde{x}_2$ $(x_2/\delta_{0.5})$" on p. 249 uniquely as $\tilde{x}_2 = x_2/\delta_{0.5}$ and the fact that indeed from their defining relation *Eq. (3.6)* along with *Eqs. (4.8)-(4.9)* the more general result $\tilde{x}_2 = c \cdot x_2/\sqrt{t - t_0}$ (where c is an arbitrary integration constant) can be obtained, it seems more than likely that ultimately the correct explicit expression for $\tilde{x}_2$ was used. The issue was that in the earlier version the indefiniteness of the integral in *Eq. (3.6)* was not fully recognized, thus the integration fell short a constant. Hence, the earlier criticism here that a mislabelling has occurred is removed. Yet, it should be noted that this correction has no effect on any of the comments ***(1)-(6)*** made before.

A. The general restrictions from the mass flux constraint

Imposing the mass flux constraint to be an invariant constraint on the general invariant solution (2.4), i.e., imposing

$$c = \int_{-\infty}^{\infty} \overline{U}_1 dx_2 = \int_{-\infty}^{\infty} \overline{U}_1^* dx_2^*, \tag{A.1}$$

where c is the global invariant constant in space and time, and where the '*'-symbol refers to the variable transformation generated by (2.4), which in infinitesimal form can be read-off from (2.4) as

$$t^* = t + \epsilon F_1(t), \quad x_2^* = x_2 + \epsilon \mathcal{F}_2(t, x_2), \quad \overline{U}_1^* = \overline{U}_1 + \epsilon\Big(a_1 \overline{U}_1 - \overline{U}_1 \partial_{x_2} \mathcal{F}_2(t, x_2) + \mathcal{F}_3(t, x_2)\Big), \tag{A.2}$$

where $\epsilon \ll 1$ is the infinitesimal parameter, (A.1) will impose natural restrictions on (A.2) and thus overall on (2.4). As can be easily verified, by performing a Taylor expansion around $\epsilon = 0$ and neglecting all higher order terms than linear in ϵ, the inverse transformation of (A.2) is given by

$$t = t^* - \epsilon F_1(t^*), \quad x_2 = x_2^* - \epsilon \mathcal{F}_2(t^*, x_2^*), \quad \overline{U}_1 = \overline{U}_1^* - \epsilon\Big(a_1 \overline{U}_1^* - \overline{U}_1^* \partial_{x_2^*} \mathcal{F}_2(t^*, x_2^*) + \mathcal{F}_3(t^*, x_2^*)\Big). \tag{A.3}$$

The restrictions then follow as

$$\begin{aligned}
0 &= c - \int_{-\infty}^{\infty} \overline{U}_1^* dx_2^* \\
&= c - \int_{-\infty}^{\infty} \Big(\overline{U}_1 + \epsilon(a_1 \overline{U}_1 - \overline{U}_1 \partial_{x_2} \mathcal{F}_2(t, x_2) + \mathcal{F}_3(t, x_2))\Big)\Big(1 + \epsilon \partial_{x_2} \mathcal{F}_2(t, x_2)\Big) dx_2 + \mathcal{O}(\epsilon^2) \\
&= \underbrace{c - \int_{-\infty}^{\infty} \overline{U}_1 dx_2}_{=0} + \epsilon \int_{-\infty}^{\infty} \Big(a_1 \overline{U}_1 - \overline{U}_1 \partial_{x_2} \mathcal{F}_2(t, x_2) + \mathcal{F}_3(t, x_2) + \overline{U}_1 \partial_{x_2} \mathcal{F}_2(t, x_2)\Big) dx_2 + \mathcal{O}(\epsilon^2) \\
&= \epsilon \int_{-\infty}^{\infty} \Big(a_1 \overline{U}_1 + \mathcal{F}_3(t, x_2)\Big) dx_2 + \mathcal{O}(\epsilon^2),
\end{aligned} \tag{A.4}$$

which for all configurations $\overline{U}_1$ can only be solved if $a_1 = 0$ and if $\mathcal{F}_3$ is an antisymmetric function in x_2, i.e., if $\int_{-\infty}^{\infty} \mathcal{F}_3(t, x_2) dx_2 = 0$, for all $t \geq 0$.

Interesting to examine is whether further restrictions will surface when considering the original differential consequence of (A.1), namely when imposing the original invariant differential constraint

$$0 = \int_{-\infty}^{\infty} \partial_t \overline{U}_1 dx_2 = \int_{-\infty}^{\infty} \partial_{t^*} \overline{U}_1^* dx_2^*. \tag{A.5}$$

This will lead to

$$\begin{aligned}
0 &= \int_{-\infty}^{\infty} \partial_{t^*} \overline{U}_1^* dx_2^* \\
&= \int_{-\infty}^{\infty} \Big[\Big((1 - \epsilon \partial_t F_1) \cdot \partial_t - \epsilon \partial_t \mathcal{F}_2 \cdot \partial_{x_2}\Big)\Big(\overline{U}_1 + \epsilon(a_1 \overline{U}_1 - \overline{U}_1 \partial_{x_2} \mathcal{F}_2 + \mathcal{F}_3)\Big)\Big]\Big(1 + \epsilon \partial_{x_2} \mathcal{F}_2\Big) dx_2 + \mathcal{O}(\epsilon^2) \\
&= \epsilon \int_{-\infty}^{\infty} \Big(- \partial_t F_1 \partial_t \overline{U}_1 - \partial_t \mathcal{F}_2 \partial_{x_2} \overline{U}_1 + a_1 \partial_t \overline{U}_1 - \overline{U}_1 \partial_{tx_2}^2 \mathcal{F}_2 + \partial_t \mathcal{F}_3\Big) dx_2 + \mathcal{O}(\epsilon^2) \\
&\underset{\text{p.Int.}}{=} -\epsilon\, \partial_t F_1(t) \underbrace{\int_{-\infty}^{\infty} \partial_t \overline{U}_1\, dx_2}_{=0} + \epsilon\, \partial_t \underbrace{\int_{-\infty}^{\infty} (a_1 \overline{U}_1 + \mathcal{F}_3)\, dx_2}_{=0 \text{ (A.4)}} = 0,
\end{aligned} \tag{A.6}$$

saying that no further restrictions exist besides those already determined from (A.4).

B. The causality principle as a modelling guideline for invariant turbulent scaling

The question is, does the particular equivalence solution (3.2), chosen from an unclosed and thus infinite set of possible equivalence transformations (2.13), have a physical justification? Or asked differently, does this solution maybe violate an underlying physical principle so that it has to be ruled out as a possible candidate? One such principle to be checked is that of cause and effect. Because, if (3.2) emerges as an equivalence invariance on the statistical level, then there must be at least a cause on the instantaneous (fluctuating) level such that (3.2) can emerge as an effect on the statistical level. Obviously, the cause need not to be an invariant itself in order to induce an invariance of the statistical Navier-Stokes equations, simply because a mean field equation can have an invariant structure that need not to exist for its underlying fluctuating equation (for further details, see e.g. Frewer *et al.* (2015, 2016, 2017) and the references therein).

The most simplest possible cause that exists as to induce the statistical invariance (3.2), which in its non-infinitesimal and one-parametrical Lie-group form reads [†]

$$\left.\begin{aligned}
&t^* = e^{\epsilon}(t-t_0)+t_0, \quad x_2^* = e^{\frac{1}{2}\epsilon}x_2, \quad \overline{U}_1^* = e^{-\frac{1}{2}\epsilon}\overline{U}_1,\\
&H_{12}^{0\,*} = e^{-\epsilon}H_{12}^0, \quad H_{ii}^{0\,*} = e^{-\epsilon}H_{ii}^0 + \frac{2\alpha_i(e^{-\epsilon/2}-e^{-\epsilon})}{\sqrt{t-t_0}}e^{-\frac{\beta x_2^2}{t-t_0}},\\
&H_{122}^{0\,*} = e^{-\frac{3}{2}\epsilon}H_{122}^0 + \overline{U}_1\frac{2\alpha_2(e^{-\epsilon}-e^{-3\epsilon/2})}{\sqrt{t-t_0}}e^{-\frac{\beta x_2^2}{t-t_0}} - \int_0^{\epsilon} d\epsilon'\Big(\mathcal{G}_1(t^{*\prime},x_2^{*\prime}) - \mathcal{F}_6(t^{*\prime},x_2^{*\prime})\Big),\\
&H_{ii2}^{0\,*} = e^{-\frac{3}{2}\epsilon}H_{ii2}^0 - \int_0^{\epsilon} d\epsilon'\Big(2\delta_{i2}\mathcal{G}_2(t^{*\prime},x_2^{*\prime}) - \mathcal{F}_{7,i,0}(t^{*\prime},x_2^{*\prime})\Big),\\
&\overline{PU_1}^{0\,*} = e^{-\frac{3}{2}\epsilon}\overline{PU_1}^0 - \overline{U}_1\frac{2\alpha_2(e^{-\epsilon}-e^{-3\epsilon/2})}{\sqrt{t-t_0}}e^{-\frac{\beta x_2^2}{t-t_0}} + \int_0^{\epsilon} d\epsilon'\,\mathcal{G}_1(t^{*\prime},x_2^{*\prime}),\\
&\overline{PU_2}^{0\,*} = e^{-\frac{3}{2}\epsilon}\overline{PU_2}^0 + \int_0^{\epsilon} d\epsilon'\,\mathcal{G}_2(t^{*\prime},x_2^{*\prime}),
\end{aligned}\right\} \tag{B.1}$$

is to transform the four space-time coordinates and the four instantaneous field variables of the deterministic Navier-Stokes equations as follows: [‡]

$$t^* = e^{\epsilon}(t-t_0)+t_0, \quad x_2^* = e^{\frac{1}{2}\epsilon}x_2, \quad U_i^* = e^{-\frac{1}{2}\epsilon}U_i + \gamma_i(t,x_2,\epsilon), \quad P^* = e^{-\epsilon}P + \gamma_P(t,x_2,\epsilon), \tag{B.2}$$

where the γ_i are three random fields with zero mean, γ_P a random field with a non-zero mean, and where all of these four random fields are to all orders statistically independent of the instantaneous fields U_i and P, i.e., in all, where

$$\left.\begin{aligned}
&\overline{\gamma_i} = 0, \quad \overline{\gamma_P} \neq 0,\\
&\overline{\gamma_{i_1}\cdots\gamma_{i_n}\gamma_P^k\cdot U_{j_1}\cdots U_{j_m}P^l} = \overline{\gamma_{i_1}\cdots\gamma_{i_n}\gamma_P^k}\cdot\overline{U_{j_1}\cdots U_{j_m}P^l}.
\end{aligned}\right\} \tag{B.3}$$

Now, if the fields γ_i and γ_P are realized such that their moments satisfy the relations

$$\left.\begin{aligned}
&\overline{\gamma_1\gamma_2} = 0, \quad \overline{\gamma_i^2} = \frac{2\alpha_i(e^{-\epsilon/2}-e^{-\epsilon})}{\sqrt{t-t_0}}e^{-\frac{\beta x_2^2}{t-t_0}},\\
&\overline{\gamma_1\gamma_2^2} = -\overline{\gamma_1\gamma_P} + \int_0^{\epsilon} d\epsilon'\,\mathcal{F}_6(t^{*\prime},x_2^{*\prime}), \quad \overline{\gamma_i^2\gamma_2} = -2\delta_{i2}\,\overline{\gamma_2\gamma_P} + \int_0^{\epsilon} d\epsilon'\,\mathcal{F}_{7,i,0}(t^{*\prime},x_2^{*\prime}),\\
&\overline{\gamma_P} = -\overline{\gamma_2^2}, \quad \overline{\gamma_1\gamma_P} = \int_0^{\epsilon} d\epsilon'\,\mathcal{G}_1(t^{*\prime},x_2^{*\prime}), \quad \overline{\gamma_2\gamma_P} = \int_0^{\epsilon} d\epsilon'\,\mathcal{G}_2(t^{*\prime},x_2^{*\prime}),
\end{aligned}\right\} \tag{B.4}$$

[†]Cf. Olver (1993); Bluman & Kumei (1996) on Lie's central theorem how to obtain a one- or multi-parametric Lie-group transformation from its infinitesimal generator.

[‡]Note that the instantaneous transformation (B.2) neither need to be an equivalence nor a Lie-group transformation of the deterministic Navier-Stokes equations. Further note that the other two (not listed) space coordinates in (B.2) are to be considered as invariants, i.e., they both transform invariantly: $x_1^* = x_1$ and $x_3^* = x_3$.

then the set of statistical equivalence transformations (B.1) are caused by (B.4), as can be easily verified by constructing the corresponding moments from (B.2) and recalling that for the flow case considered herein $\overline{U}_2 = \overline{U}_3 = 0$. In other words, the chosen set of equivalence transformations (B.1), or in their infinitesimal form (3.2), do not violate the classical principle of cause and effect, since at least one cause on the instantaneous level can be found, for instance (B.2)-(B.4), from which then the invariance (B.1) results as an effect on the statistical level.[†]

This is in stark contrast to the equivalence transformations *Eqs. (A1)-(A11)* chosen in Sadeghi *et al.* (2018), for which no cause of any type and form can be found. The key problem is that the transformations for the triple-velocity moments *Eqs. (A8)-(A9)* are inconsistent to ones chosen for the double-velocity moments *Eqs. (A4)-(A7)*, even when including the correct terms that are originally missing from this expression (see last footnote on p. 3): No transformation on the instantaneous level can be found as to make these two transformations consistent, and hence have to be discarded as unphysical. Let's prove this claim for the reduced version of *Eqs. (A1)-(A11)* that finally has been used by Sadeghi *et al.* (2018) to derive the Reynolds stress scalings *Eqs. (4.10)-(4.12)* and *Eq. (B5)*, namely to choose $F_3(t) = a_1 = a_{U_1} = 0$ (p. 244), $F_1(t) = D(t - t_0)$, $F_2(t) = \frac{1}{2}D$ (p. 249), and $a_{H_{12}} = 0$ (p. 255), which then reduces *Eqs. (A1)-(A11)* simply to

$$\left.\begin{aligned} &\xi_t = D(t-t_0), \qquad \xi_{x_2} = \tfrac{1}{2}Dx_2, \qquad \eta_{\overline{U}_1} = -\tfrac{1}{2}D\overline{U}_1, \\ &\eta_{H^0_{12}} = -DH^0_{12}, \qquad \eta_{H^0_{ii}} = -DH^0_{ii} + a_{H_{ii}}, \\ &\eta_{H^0_{ijk}} = -\tfrac{3}{2}DH^0_{ijk} + a_{H_{ijk}}, \qquad \eta_{\overline{PU_i}^0} = -\tfrac{3}{2}D\overline{PU_i}^0 + a_{PU_i}, \end{aligned}\right\} \tag{B.5}$$

which in its non-infinitesimal and one-parametrical Lie-group form then reads

$$\left.\begin{aligned} &t^* = e^{D\epsilon}(t-t_0) + t_0, \qquad x_2^* = e^{\frac{1}{2}D\epsilon}x_2, \qquad \overline{U}_1^* = e^{-\frac{1}{2}D\epsilon}\overline{U}_1, \\ &H^{0*}_{12} = e^{-D\epsilon}H^0_{12}, \qquad H^{0*}_{ii} = e^{-D\epsilon}H^0_{ii} + (1-e^{-D\epsilon})\frac{a_{H_{ii}}}{D}, \\ &H^{0*}_{ijk} = e^{-\frac{3}{2}D\epsilon}H^0_{ijk} + \tfrac{2}{3}(1-e^{-\frac{3}{2}D\epsilon})\frac{a_{H_{ijk}}}{D}, \qquad \overline{PU_i}^{0*} = e^{-\frac{3}{2}D\epsilon}\overline{PU_i}^0 + \tfrac{2}{3}(1-e^{-\frac{3}{2}D\epsilon})\frac{a_{PU_i}}{D}. \end{aligned}\right\} \tag{B.6}$$

To search for a cause for this equivalence, the most general ansatz, that can be made to induce (B.6) from an instantaneous transformation, is

$$\left.\begin{aligned} t^* = e^{D\epsilon}(t-t_0) + t_0, \qquad x_2^* = e^{\frac{1}{2}D\epsilon}x_2, \\ U_i^* = e^{-\frac{1}{2}D\epsilon}U_i + f_i(t,x_2,U_1,U_2,U_3,P,\epsilon), \qquad P^* = e^{-\epsilon D}P + f_P(t,x_2,U_1,U_2,U_3,P,\epsilon), \end{aligned}\right\} \tag{B.7}$$

where in a first step, due to aiming at the most general ansatz, no prior restrictions or assumptions are made on the four functionals f_i and f_P. Now, in order to induce the transformations in (B.6) say, for example, for the mean velocity $\overline{U}_1$ and the double-velocity moment H^0_{11}, the moments for f_1 have to satisfy

$$\overline{f_1} = 0, \qquad 2e^{-\frac{1}{2}D\epsilon}\overline{U_1 f_1} + \overline{f_1^2} = (1-e^{-D\epsilon})\frac{a_{H_{11}}}{D}. \tag{B.8}$$

But now, since for any particular realization of the instantaneous functional f_1, the above three moments will be functionals of velocity and pressure moments up to the order specified by f_1, i.e.,

[†]Worthwhile to note is that finding a particular realization or the associated probability distribution function (PDF) to the random functions γ_i and γ_P from the knowledge of their moments (B.4) is a challenging inverse problem, in particular as a solution is not necessarily unique and for which, thus, further fundamental physical constraints have to be placed: See e.g. Bandyopadhyay *et al.* (2005); Biswas & Bhattacharya (2010) in reconstructing a single PDF from its moments up to a certain finite order by using a maximum entropy approach. Here, in this comment, as well as e.g. in She *et al.* (2017); Chen *et al.* (2018), an explicit realization of the random field transformations are not needed to determine turbulent scaling invariants. Here, the only thing to look out for is that the induced moment relations (B.4) do not contradict each other.

since for any particular realization of f_1 (B.7) we would have the following induced realization

$$\left.\begin{aligned} \overline{f_1} &= \Theta_{1,1}(t, x_2, \epsilon, \overline{U}_i, \overline{P}, H^0_{ij}, H^0_{ijk}, \overline{PU_i}, \dots), \\ \overline{U_1 f_1} &= \Theta_{1,2}(t, x_2, \epsilon, \overline{U}_i, \overline{P}, H^0_{ij}, H^0_{ijk}, \overline{PU_i}, \dots), \\ \overline{f_1^2} &= \Theta_{1,3}(t, x_2, \epsilon, \overline{U}_i, \overline{P}, H^0_{ij}, H^0_{ijk}, \overline{PU_i}, \dots), \end{aligned}\right\} \tag{B.9}$$

the above relations (B.8) inherently will turn into algebraic restrictions for velocity and pressure moments, which, certainly, is not what to be aimed at, simply because these restrictions are algebraic equations then, which unnaturally will augment the defining set of moment equations (2.1) and therefore will alter the systems' invariant property as originally given by (B.6), or in its infinitesimal form by (B.5). This negative and destructive feedback property onto the original system (2.1) can only be avoided if one demands for the instantaneous functionals f_i and f_P not only full independence of the instantaneous fields U_i and P but also, up to all orders, their statistical independence to them if chosen as random functions, i.e.,[†]

$$\left.\begin{aligned} & f_i(t, x_2, U_1, U_2, U_3, P, \epsilon) \equiv \sigma_i(t, x_2, \epsilon), \qquad f_P(t, x_2, U_1, U_2, U_3, P, \epsilon) \equiv \sigma_P(t, x_2, \epsilon), \\ & \text{and:} \quad \overline{\sigma_{i_1} \cdots \sigma_{i_n} \sigma_P^k \cdot U_{j_1} \cdots U_{j_m} P^l} = \overline{\sigma_{i_1} \cdots \sigma_{i_n} \sigma_P^k} \cdot \overline{U_{j_1} \cdots U_{j_m} P^l}. \end{aligned}\right\} \tag{B.10}$$

Turning back to our original aim to induce (B.6) from (B.7), along with its consistency constraint (B.10), we now get the following relations for the moments of σ_i

$$\overline{\sigma_i} = 0, \qquad \overline{\sigma_1 \sigma_2} = 0, \qquad \overline{\sigma_i^2} = (1 - e^{-D\epsilon}) \frac{a_{H_{ii}}}{D}, \tag{B.11}$$

when considering the transformations for the mean velocity $\overline{U}_1$ and the double-velocity moments H^0_{ij} in (B.6), while when considering and including also the triple-velocity and pressure-velocity moments, the above set of relations (B.11) gets augmented by

$$\overline{\sigma_i \sigma_j} = 0, \qquad \overline{\sigma_i \sigma_j \sigma_k} = \tfrac{2}{3}(1 - e^{-\frac{3}{2} D\epsilon}) \frac{a_{H_{ijk}}}{D}, \qquad \overline{\sigma_P} = 0, \qquad \overline{\sigma_P \sigma_i} = \tfrac{2}{3}(1 - e^{-\frac{3}{2} D\epsilon}) \frac{a_{PU_i}}{D}. \tag{B.12}$$

However, if we demand $\epsilon \neq 0$ or $a_{H_{ii}} \neq 0$ as in Sadeghi *et al.* (2018), then the zero-result for the three diagonal double-moments obtained in (B.12), namely $\overline{\sigma_i^2} = 0$, stands in contradiction to the non-zero result $\overline{\sigma_i^2} \neq 0$ obtained in (B.11). This contradiction can only be solved, either if we allow for no transformations at all, i.e., by putting the group parameter $\epsilon = 0$, or if we allow for no translations in the diagonal double-velocity moments, i.e., by putting $a_{H_{ii}} = 0$, which thus would directly and analytically prove that the non-zero translation parameters presented in *Tab. 1* in Sadeghi *et al.* (2018) are all unphysical. Hence, in either way, no cause on the instantaneous level (B.7) can be generated, such that the statistical invariance (B.6) for $a_{H_{ii}} \neq 0$ can emerge as an effect. □

[†]As was already stressed in Frewer *et al.* (2017), yet for a different setting, the randomness of σ_i and σ_P defined in (B.10), as well as that of γ_i and γ_P in (B.2), is of a different origin and nature than the randomness of the field variables U_i and P. Hence, a consistent random field transformation can only be performed if it occurs statistically independent to the field variables it transforms, otherwise the structure of the original statistical field equations will alter and thus will be different from the usual textbook equations. For more details on random field transformations, see e.g. Filipiak (1992); McComb (2014), where in particular the peculiarities and difficulties of the random Galilean transformations are discussed, explicitly showing that random field transformations are ensemble type of operations and not kinematical operations.

References

Bandyopadhyay, K., Bhattacharya, A. K., Biswas, P. & Drabold, D. A. 2005 Maximum entropy and the problem of moments: A stable algorithm. *Phys. Rev. E* **71** (5), 057701.

Biswas, P. & Bhattacharya, A. K. 2010 Function reconstruction as a classical moment problem: A maximum entropy approach. *J. Phys. A: Math. Theor.* **43** (40), 405003.

Bluman, G. W. & Kumei, S. 1996 *Symmetries and Differential Equations*. Springer Verlag.

Bradbury, L. J. S. 1965 The structure of a self-preserving turbulent plane jet. *J. Fluid Mech.* **23** (1), 31–64.

Chen, X., Hussain, F. & She, Z.-S. 2018 Quantifying wall turbulence via a symmetry approach. Part 2. Reynolds stresses. *J. Fluid Mech.* **850**, 401–438.

Filipiak, M. 1992 Further assessment of the LET theory. PhD thesis, The University of Edinburgh.

Frewer, M. & Khujadze, G. 2016 On the use of applying Lie-group symmetry analysis to turbulent channel flow with streamwise rotation. *arXiv:1609.08155*.

Frewer, M., Khujadze, G. & Foysi, H. 2014*a* Is the log-law a first principle result from Lie-group invariance analysis? A comment on the Article by Oberlack (2001). *arXiv:1412.3069*.

Frewer, M., Khujadze, G. & Foysi, H. 2014*b* On the physical inconsistency of a new statistical scaling symmetry in incompressible Navier-Stokes turbulence. *arXiv:1412.3061*.

Frewer, M., Khujadze, G. & Foysi, H. 2015 Comment on "Statistical symmetries of the Lundgren-Monin-Novikov hierarchy". *Phys. Rev. E* **92** (6), 067001.

Frewer, M., Khujadze, G. & Foysi, H. 2016 A note on the notion "statistical symmetry". *arXiv:1602.08039*.

Frewer, M., Khujadze, G. & Foysi, H. 2017 Comment on 'Lie symmetry analysis of the Lundgren-Monin-Novikov equations for multi-point probability density functions of turbulent flow'. *arXiv:1710.00669*.

McComb, W. D. 2014 *Homogeneous, Isotropic Turbulence: Phenomenology, Renormalization and Statistical Closures*. Oxford University Press.

Olver, P. J. 1993 *Applications of Lie Groups to Differential Equations*. Springer Verlag.

Sadeghi, H., Oberlack, M. & Gauding, M. 2018 On new scaling laws in a temporally evolving turbulent plane jet using Lie symmetry analysis and direct numerical simulation. *J. Fluid Mech.* **854**, 233–260.

She, Z.S., Chen, X. & Hussain, F. 2017 Quantifying wall turbulence via a symmetry approach: a Lie group theory. *J. Fluid Mech.* **827**, 322–356.

Vu, K. T., Jefferson, G. F. & Carminati, J. 2012 Finding higher symmetries of differential equations using the MAPLE package DESOLV-II. *Comp. Phys. Comm.* **183** (4), 1044–1054.